# Numerical Study of Natural Convection of Newtonian Fluid within a Square Cavity using a Flexible fin

**MEDJEDED Afafe [1], DERRAZ Hanaa [2], BENCHERIF Atika [3], BOUZIT Mohamed [4]**

[1,2,3,4] *Lab of of Maritime Sciences and Engineering LSIM Faculty of Mechanical Engineering, University of Science and Technology of Oran, Mohamed Boudiaf; P.B 1505 El Mnaouar 31000 Oran Algeria*

*E-mail:* afafe.medjeded@univ-usto.dz , Atika.bencherif@univ-usto.dz , hanaa.derraz@univ-usto.dz , mohamed.bouzit@univ-usto.dz .

**Abstract**: In this study, the flow and heat transfer of a Newtonian power fluid in a cavity square is discussed. The top and bottom walls of the cavity are well insulated. the left vertical wall is at a hot temperature, and the right wall is at a cold temperature. A flexible elastic fin is fixed in the middle of the wall in different positions (left, right). The fluid-structure interaction (FSI) in the cavity and the hot fins and Newtonian fluid are combined. The interaction of the flow with the fin leads to the deformation of the fin and the change of the fin position modifies the flow and the heat transfer. The arbitrary Lagrangian-Eulerian (ALE) method with the moving mesh method is employed to model the deflection of the structure within the fluid domain. The finite element method is adopted to solve the governing equations, the parameters studied are the power law index, the Rayleigh number $(10^3 < Ra < 10^5)$ , the elasticity modulus$(5.10^9 < Et < 10^{11})$, Prandtl number (10).isotherms and streamlines and the average Nusselt number are studied. Results obtained in this study that increasing the Rayleigh number leads to an increase in the average Nusselt number, which is associated with a higher Rayleigh number. Therefore, it was found that a square cavity can increase the heat transfer rate.

*Keywords*: Natural convection; square cavity; Flexible fin; Newtonian fluid; FSI.

## 1. INTRODUCTION

Due to uneven temperatures within enclosures and the presence of buoyancy forces, a process called natural convective heat transfer plays an important role in various fields such as electronic component cooling, double pane windows, and nuclear reactor cooling systems. This essential process enables the transfer of heat within engineering systems, and relies on the natural flow of buoyancy forces. Considering the natural convection of Newtonian fluids, many studies have investigated the transient natural convection of vibrating flexible fins, The effet of fluid-solid interaction on transient natural convection inside a square cavity is presented by " Gangawane, K. M., & Manikandan, B. (2017) " , It is found that the overall rate of heat transfer increases exponentially with the rise of the oscillation amplitude and an oscillation amplitude of 0.1 could result in 3.4 percent improvement in the heat transfer rate, the average Nusselt number is found higher for Darcy number compared with Darcy-Forchheimer model for all studied Rayleigh numbers. The natural convection heat transfer in a square cavity wherein the buoyancy-induced flow by a thin flexible heater-plate is generated by "Gilmanov, A., Le, T. B., & Sotiropoulos, F. (2015) ". Therefore, the problem of unsteady fluid structure interaction inside different cavities have been investigated in many published works such as, square cavity ("Hakim, M. A., Ahad, A. I., Karim, A. U., Saha, S., & Hasan, M. N. (2022)", "Ismael, M. A., & Jasim, H. F. (2018). ", " Jain, S. R., Subhani, S., & Kumar, R. S. (2022) ".) , L-shaped enclosure " Kebriti, S., & Moqtaderi, H. (2021) ". It is observed that the 45° angle of rotation square cylinder provides the most optimum and efficient of heat transfer at higher Rayleigh number. The unsteady natural convection heat transfer inside an enclosure with a heated circular cylinder have been investigated in the literature ("Khanafer, K., & Vafai, K. (2020) ", " Loenko, D. S., Shenoy, A., & Sheremet, M. A. (2021) ".) , In other studies, regarding the mixed convection of Newtonian fluid inside many enclosures such as, a square cavity having two inlet and outlet opening "Makayssi, T., Lamsaadi, M., & Kaddiri, M. (2021) ", a square cavity having a flexible side wall " Mehryan, S. A. M., Alsabery, A., Modir, A., Izadpanahi, E., & Ghalambaz, M. (2020) ". rectangular enclosure ("Saleh, H., Naganthran, K., Hashim, I., Ghalambaz, M., & Nazar, R. (2022)", "Salehpour, A., Abdolahi Sadatlu, M. A., & Sojoudi, A. (2019)") it is found that as flow behaviour index increases for a flow with a given Rayleigh number, average Nusselt number at hot wall and the rate of melting decrease. The heat transfers and flow characteristics of natural convection from a hot cylinder body in a square enclosure is investigated by "Subhani, S., & Kumar, R. S. (2022)". The compressible B-spline material point method (WC-BSMPM) to resolve the complicated free surface flow of non-Newtonian fluid with a power law rheology model is provided and extended by "Shahabadi, M., Mehryan, S. A. M., Ghalambaz, M., & Ismael, M. (2021)".

*1.1 Modelling approach*

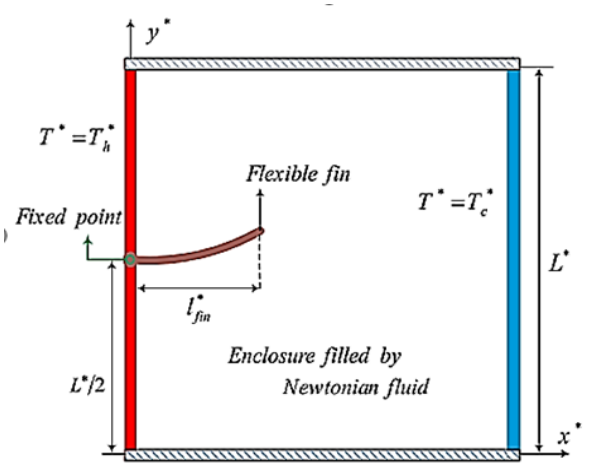


Figure 1. Physical model of convection in a cavity with a flexible fin and coordinate system

## 2. FUNDAMENTAL RELATIONS

*2.1 Governing equations*

Continuity equation:

$$\boldsymbol{\nabla}^* \ \boldsymbol{u}^* = 0 \qquad (1)$$

Momentum equations:

$$\rho_f \left[\frac{\partial u^*}{\partial t} + (\boldsymbol{u}^* - \boldsymbol{w}^*)\nabla^* u^*\right] - \nabla^*[-P^* I + u(\boldsymbol{\nabla}^*\boldsymbol{u}^* + (\boldsymbol{\nabla}^*\boldsymbol{u}^*)^{tr})] - \rho_f \beta_{\boldsymbol{g}}(T^* - T_c^*) = 0 \qquad (2)$$

The energy equation for the fluid:

$$(\rho\, c_p)_f \left[\frac{\partial T^*}{\partial t} + (\boldsymbol{u}^* - \boldsymbol{w}^*)\cdot \boldsymbol{\nabla}^* T^*\right] - k_f \boldsymbol{\nabla}^{*2} T^* = 0 \qquad (3)$$

For elastic structure domain:

The equations of the nonlinear elastic displacement and the energy of the fin can be written as:

$$\rho_s \frac{d^2 \boldsymbol{d}_s^*}{dt^2} - \nabla^* \sigma^* = \boldsymbol{F}_v^* \qquad (4)$$

The energy equation for the flexible fin:

$$(\rho c_p)\frac{\partial T^*}{\partial t} - k_s \nabla^{*2} T^* = 0 \qquad (5)$$

$P^*$ and $T^*$ as the pressure of the fluid and temperature of the solid/ fluid, respectively, g the gravity acceleration. $\boldsymbol{\sigma}^*$ shows the solid stress tensor. $\mathbf{d}_s^*$ denotes the displacement vector of the fin so that $d\mathbf{d}_s^*/dt = \boldsymbol{w}^*$ and $\boldsymbol{F}_v^*$ indicates the body force imposed on the flexible fin. $\boldsymbol{\rho}$ indicates the density where f and s mention to the fluid and solid, respectively. $\alpha_f$ is thermal diffusivity of the fluid, $\alpha_s$is the kinematic viscosity, and $\beta$ shows the volumetric thermal expansion coefficient of the fluid. The Neo-Hookean solid model is applied to express the stress tensor of Eq. (4):

$$\boldsymbol{\sigma}^* = J^{-1} F S F^{tr} | F = (I + \boldsymbol{\nabla}^* \boldsymbol{d}_s^*), J = det(F) \ \& \ \mathrm{S} = \partial W_s / \partial \varepsilon \qquad (6)$$

$$W_s = \frac{1}{2} l(J^{-1} I_1 - 3) - l \ln(J) + \frac{1}{2}\lambda(\ln(J))^2$$
$$l = E/\big(2(1+v)\big)$$
$$\lambda = Ev/\big((1+v)(1-2v)\big) \qquad (7)$$

$$\varepsilon = \frac{1}{2}(\boldsymbol{\nabla}^* \boldsymbol{d}_s^* + \boldsymbol{\nabla}^* \boldsymbol{d}_s^{*tr} + \boldsymbol{\nabla}^* \boldsymbol{d}_s^{*tr} \boldsymbol{\nabla}^* \boldsymbol{d}_s^*) \qquad (8)$$

*2.2 Boundary conditions*

The boundary conditions useful to the external walls and the interface of the flexible fin can be written as:

at the hot wall:

$$T^* = T_h^* , u^* = \ v^* = 0 \qquad (9)$$

at the cold wall:

$$T^* = T_c^* , u^* = \ v^* = 0 \qquad (10)$$

at the interface of the flexible fin:

$$k_f \frac{\partial y}{\partial x}\Big|_f = k_s \frac{\partial y}{\partial x}\Big|_s \qquad (11)$$

Also, the Rayleigh and Prandtl numbers and the Elasticity modulus are introduced as:

$$Ra = \frac{\rho_0^2 \, c_p g \beta \Delta T d^3}{\mu_B k} \qquad (12)$$

$$Pr = \frac{c_p \mu_B}{k} \qquad (13)$$

$$E_\tau = \frac{E \cdot 2R^{*2}}{\rho_f \alpha_f^2} \qquad (14)$$

The non-dimensionless heat transfer rates through the fluid intimate to the hot wall with the flexible fin basis are, respectively:

$$Nu_f = -\frac{\partial \theta}{\partial X} \qquad (15)$$

$$Nu_s = -k_r \frac{\partial \theta}{\partial X} \qquad (16)$$

The average Nusselt number at the hot wall is also introduced as:

$$\overline{Nu} = \int_0^{s_1} Nu_f \ d_y + \int_{s_1}^{s_2} Nu_s \ d_y + \int_{s_2}^{1} Nu_f \ d_y \Big| \begin{matrix} s_1 = \frac{1}{2} - \frac{\boldsymbol{t}_{fin}}{2} \\ s_2 = \frac{1}{2}\frac{\boldsymbol{t}_{fin}}{2} \end{matrix} \qquad (17)$$

*2.3 Nomenclature*

| | |
|---|---|
| $E$ | times |
| $f$ | Frequency |
| $\boldsymbol{F_v}$ | vector of volume force |
| $\boldsymbol{g}$ | gravity vector |
| $R$ | characteristic size (enclosure high and width) |
| $Pr$ | Prandtl number |
| $Ra$ | Rayleigh number |
| $t$ | time in dimensional form |
| $T$ | temperature field |
| $\boldsymbol{u}$ | velocity vector |
| $\boldsymbol{w}$ | the moving mesh velocity vector |
| $x, y$ | Cartesian coordinates |

**Greek symbols**

| | |
|---|---|
| $\alpha$ | coefficient of the thermal diffusivity |
| $\beta$ | coefficient of the volumetric thermal expansion |
| $\mu$ | the fluid's dynamic viscosity |
| $\nu$ | Poisson's ratio |
| $\rho$ | Density |
| $\rho_R$ | the ratio of fluid to solid-structure density |
| $\tau o$ | Fluid yield stress |

**Subscripts**

| | |
|---|---|
| $avrg$ | the average property |
| $c$ | the cold Wall |
| $f$ | the fluid property |
| $h$ | the hot property |
| $s$ | the flexible plate |

**Superscripts**

| | |
|---|---|
| $tr$ | matrix transpose |
| $*$ | dimensional for of variables and parameters |

## 3. FUNDAMENTAL RELATIONS

*3.1 Validation*

Another critical step in the simulation to ensure the accuracy and correctness of the obtained results is the validation through other studies. This work is validated on basis of a study done by Mohammad Shahabadi.

First, the contours of isotherms reported by Mohammad Shahabadi when Pr=10 and Et=$10^{10}$ have been used for the validation of this study. As showed in the Fig. 3, the present numerical results thoroughly competition with literature of Shahabadi.

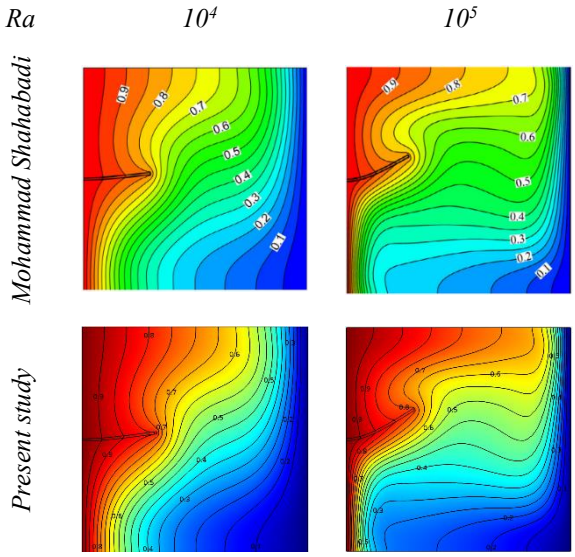


Figure 2. Comparing between the results of the present study and the contours of isotherms reported by Mohammad Shahabadi when Pr=10 and Et=$10^{10}$

Second, streamlines reported by Mohammad Shahabadi when Pr=10 and Et=$10^{10}$ are compared for different Rayleigh number with the present study Fig. 3, the obtained results of the chosen Ra of this study and Shahabadi are showed a suitable agreement.

Finally, for validation of the natural convection mechanism of a Newtonian fluid within a cavity, the Shahabadi numerical modeling has been re-simulated by the code employed in the present study. The evaluation of the Nusselt number for different values of Rayleigh number is represented in the Table 1, there exists suitable agreement between the results of the current model and the results found Shahabadi.

**Table 1. The average Nusselt (Nu) for different Rayleigh number at Pr =10**

| Ra | $Nu_{avg}$ | | |
|---|---|---|---|
| | Mohammad Shahabadi | Present study | Error % |
| $10^3$ | 1.08949 | 1.12423 | 3,474 |
| $10^4$ | 1.93385 | 1.92536 | 0,849 |
| $10^5$ | 4.41245 | 4.41632 | 0,387 |

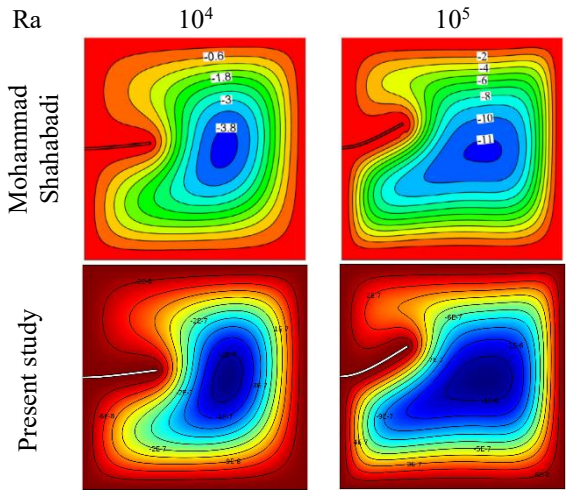


Figure 3. Comparing between the results of the present study and the contours of isotherms reported by Mohammad Shahabadi when Pr=10 and Et=$10^{10}$

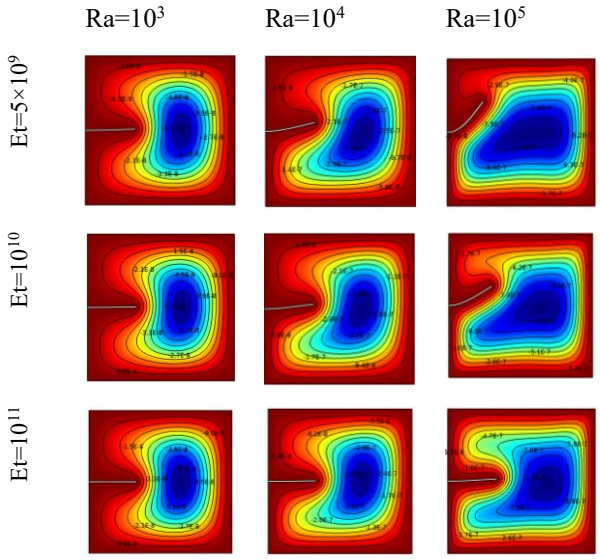


Figure 5. Streamlines contours for various Rayleigh number (Ra) and different values of elasticity modulus (Et) at Pr=10.

## 4. RESULTS AND DISCUSSION

Figures 4 and 5 show the contours of the isotherms and streamlines for different Rayleigh numbers (Ra) and elasticity at Pr = 10, position 1 (left). It can be seen that increasing the Rayleigh number has a significant effect on the flow configuration, notably by increasing recirculation. On the other hand, varying the elasticity has little influence on the flow configuration, but it does have a considerable impact on fin deformation, especially at low elasticity numbers.Note that maximum deformation is observed at Ra = $10^5$ and Et = 5 × $10^9$; an increase in elasticity makes the fin stiffer, thus reducing deformation.

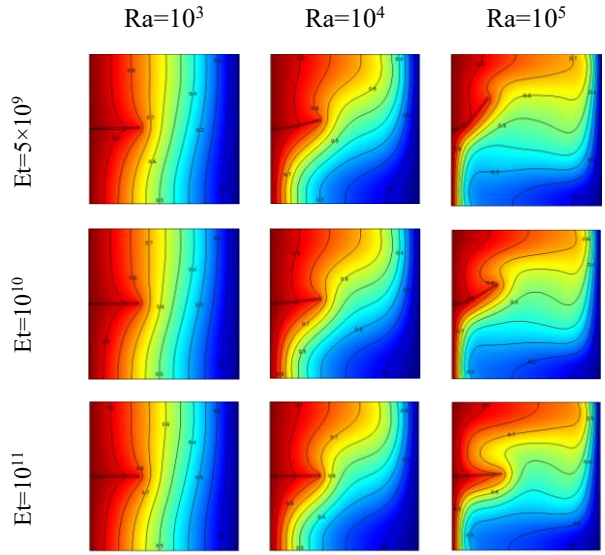


Figure 4. Isotherms contours for various Rayleigh number (Ra) and different values of elasticity modulus (Et) at Pr=10.

Figures 6 and 7 show the contours of the isotherms and streamlines for different Rayleigh and elasticity numbers at Pr = 10, position 2(right) ., where the fin is moved from the hot to the cold wall. Several significant differences can be observed: firstly, the variation in Rayleigh number does not appear to be as critical as for the previous position (position 1). As far as fin deformation is concerned, it is remarkable that the direction of deformation changes as a function of position.

Specifically, when the fin is attached to the hot wall, it deforms upwards, whereas when it is attached to the cold wall, it deforms in the opposite direction, i.e. downwards. Nevertheless, maximum deformation is always observed at Ra = $10^5$ and Et = 5 × $10^9$.

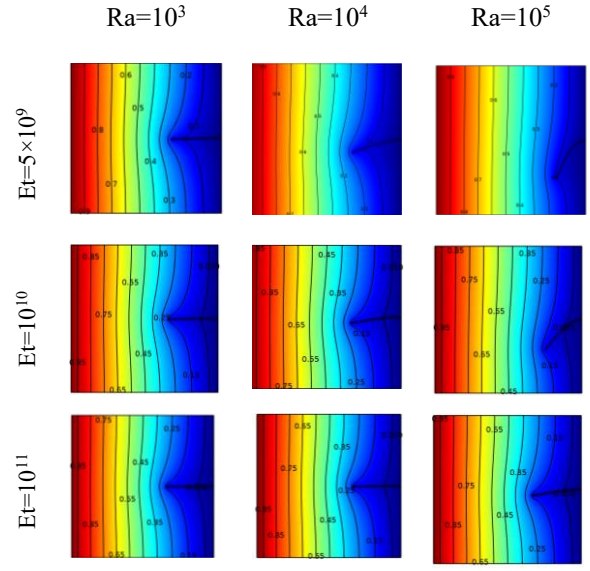


Figure 6. Isotherms contours for various Rayleigh number (Ra) and different values of elasticity modulus (Et) at Pr=10 (position 2).

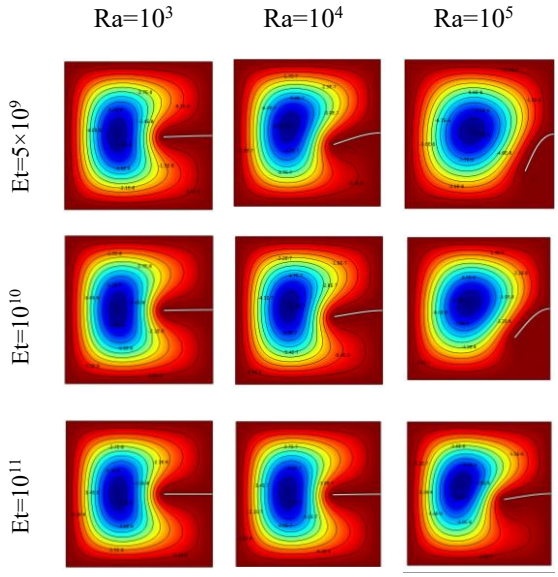


Figure 7. Streamlines contours for various Rayleigh number (Ra) and different values of elasticity modulus (Et) at Pr=10 (position 2).

The figure 8 shows the variation of the Nusselt number as a function of time for different Rayleigh numbers (Et = $10^{10}$). It can be seen that an increase in the Rayleigh number leads to an increase in the Nusselt number, indicating an increase in heat transfer.

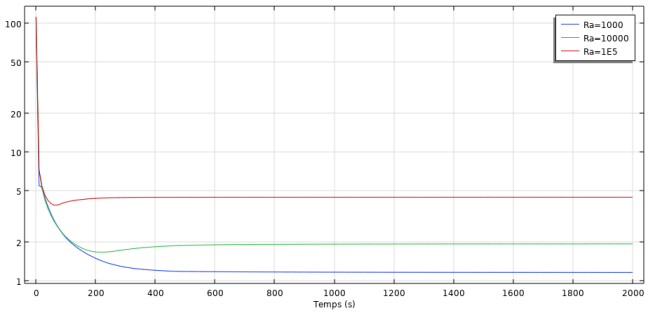


Figure 8. The variation of Nusselt number along the hot wall with for different Rayleigh number at Et=$10^{10}$ and Pr=10

The figure 9 also shows the variation of the Nusselt number as a function of time for different elastic numbers (Ra = $10^5$). It can be seen that the variation in elasticity has a negligible influence on the variation in Nusselt number, and therefore on heat transfer.

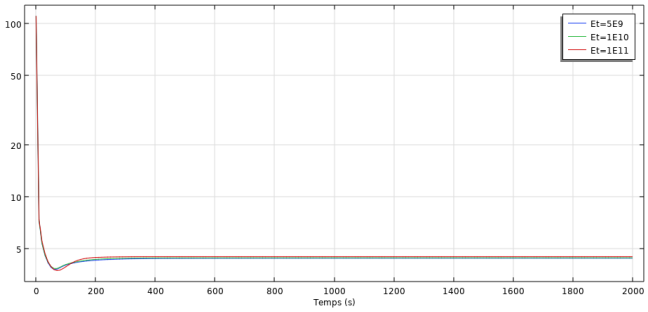


Figure 9. The variation of Nusselt number along the hot wall with time for different Elasticity modulus at Ra=$10^5$ and Pr=10

The figures 10-11 show the variation of the Nusselt number as a function of time for different Rayleigh numbers (Et = $10^{10}$) and elasticity numbers (Ra = $10^5$), by changing the position of the fin. It can be seen that the variation in Rayleigh number and elasticity number becomes negligible compared with the previous fin position.

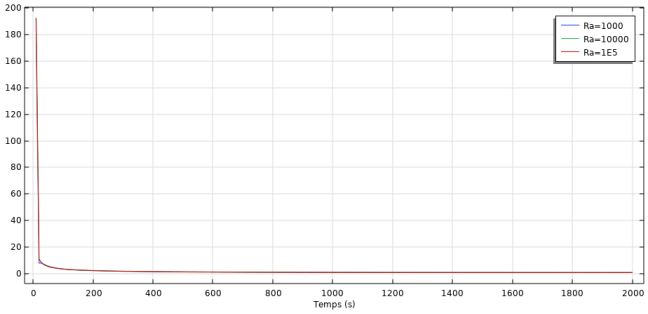


Figure 10. The variation of Nusselt number along the cold wall with for different Rayleigh number at Et=$10^{10}$ and Pr=10(position 2).

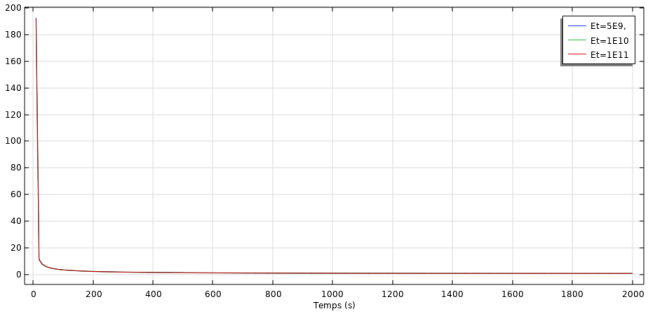


Figure 11. The variation of Nusselt number along the cold wall with time for different Elasticity modulus at Ra=$10^5$ and Pr=10 (position 2).

## 6. CONCLUSIONS

Numerical simulations were conducted to study natural convective flow of Newtonian fluids in a square enclosure using the finite element method. The study investigated the influences of Rayleigh number (Ra) and Elasticity modulus (Et) on convective flow and heat transfer. The key findings are summarized as follows:

- Initially, heat transfer is primarily through conduction in the early stages, transitioning gradually to natural convection. Buoyancy forces significantly affect the vortices formed within the cavity, particularly at higher Rayleigh numbers.

- The fin exhibits maximum deformation at steady state when elasticity modulus is low, although the average Nusselt number on the hot wall remains unaffected by elasticity modulus.

- Higher Rayleigh numbers correlate with increased intensity of convective flow, heat, and mass transfer due to reduced viscosity effects outward. However, this influence is more pronounced at high Rayleigh numbers and diminishes at extreme values.

- The square shape of the enclosure appears to enhance the overall heat transfer rate.

These results underscore the complex interplay between Rayleigh number, elasticity modulus, and heat transfer mechanisms within the square enclosure, highlighting the importance of geometric factors in enhancing heat transfer efficiency.

## REFERENCES


Gangawane, K. M., & Manikandan, B. (2017). Laminar natural convection characteristics in an enclosure with heated hexagonal block for non-Newtonian power law fluids. Chinese Journal of Chemical Engineering, 25(5), 555-571. https://doi.org/10.1016/j.cjche.2016.08.028

Gilmanov, A., Le, T. B., & Sotiropoulos, F. (2015). A numerical approach for simulating fluid structure interaction of flexible thin shells undergoing arbitrarily large deformations in complex domains. Journal of computational physics, 300, 814-843. https://doi.org/10.1016/j.jcp.2015.08.008

Hakim, M. A., Ahad, A. I., Karim, A. U., Saha, S., & Hasan, M. N. (2022). Fluid structure interaction and heat transfer enhancement with dynamic flexible flow modulator. International Communications in Heat and Mass Transfer, 134, 105983. https://doi.org/10.1016/j.icheatmasstransfer.2022.105983

Ismael, M. A., & Jasim, H. F. (2018). Role of the fluid-structure interaction in mixed convection in a vented cavity. International Journal of Mechanical Sciences, 135, 190-202. https://doi.org/10.1016/j.ijmecsci.2017.11.001

Jain, S. R., Subhani, S., & Kumar, R. S. (2022). Numerical study on performance enhancement of a square enclosure with circular cylinder of varying geometries. Journal of Thermal Analysis and Calorimetry, 1-21. https://doi.org/10.1007/s10973-021-10641-5

Kebriti, S., & Moqtaderi, H. (2021). Numerical simulation of convective non-Newtonian power-law solid-liquid phase change using the lattice Boltzmann method. International Journal of Thermal Sciences, 159, 106574. https://doi.org/10.1016/j.ijthermalsci.2020.106574

Khanafer, K., & Vafai, K. (2020). Effect of a circular cylinder and flexible wall on natural convective heat transfer characteristics in a cavity filled with a porous medium. Applied Thermal Engineering, 181, 115989. https://doi.org/10.1016/j.applthermaleng.2020.115989

Loenko, D. S., Shenoy, A., & Sheremet, M. A. (2021). Effect of time-dependent wall temperature on natural convection of a non-Newtonian fluid in an enclosure. International Journal of Thermal Sciences, 166, 106973. https://doi.org/10.1016/j.ijthermalsci.2021.106973

Makayssi, T., Lamsaadi, M., & Kaddiri, M. (2021). Natural double-diffusive convection for the Carreau shear-thinning fluid in a square cavity submitted to horizontal temperature and concentration gradients. Journal of Non-Newtonian Fluid Mechanics, 297, 104649. https://doi.org/10.1016/j.jnnfm.2021.104649

Mehryan, S. A. M., Alsabery, A., Modir, A., Izadpanahi, E., & Ghalambaz, M. (2020). Fluid-structure interaction of a hot flexible thin plate inside an enclosure. International Journal of Thermal Sciences, 153, 106340. https://doi.org/10.1016/j.ijthermalsci.2020.106340

Saleh, H., Naganthran, K., Hashim, I., Ghalambaz, M., & Nazar, R. (2022). Role of fluid-structure interaction in free convection in square open cavity with double flexible oscillating fins. Alexandria Engineering Journal, 61(2), 1217-1234. https://doi.org/10.1016/j.aej.2021.04.073

Salehpour, A., Abdolahi Sadatlu, M. A., & Sojoudi, A. (2019). Unsteady natural convection in a differentially heated rectangular enclosure possessing sinusoidal corrugated side walls loaded with power law non-Newtonian fluid. Fluid Dynamics, 54, 159-176. https://doi.org/10.1134/S0015462819010129

Subhani, S., & Kumar, R. S. (2022). Natural convection heat transfer enhancement of circular obstacle within square enclosure. Journal of Thermal Analysis and Calorimetry, 147(7), 4711-4729. https://doi.org/10.1007/s10973-021-10829-9

Shahabadi, M., Mehryan, S. A. M., Ghalambaz, M., & Ismael, M. (2021). Controlling the natural convection of a non-Newtonian fluid using a flexible fin. Applied Mathematical Modelling, 92, 669-686. https://doi.org/10.1016/j.apm.2020.11.029